POSSIBLE ATMOSPHERIC WATER VAPOR CONTRIBUTION FROM MARTIAN SWISS CHEESE TERRAIN.
A. C. Innanen[1], M. E. Landis[2], P. O. Hayne[2] and J. E. Moores[1], [1] Centre for Research in Earth and Space Science, York University, Toronto, Ontario (ainnanen@yorku.ca), [2] Laboratory for Atmospheric and Space Physics, University of Colorado, Boulder, Colorado.

Introduction: The south polar residual cap (SPRC) of Mars is a quasi-stable CO_2 ice cap that ranges in thickness from on the order of 10 m in older areas to ~1 m in younger areas [1]. The SPRC has a variety of morphological features including long, parallel depressions ('fingerprint terrain'), raised mesas, and smaller curl, heart-shaped, and quasi-circular depressions known as 'Swiss cheese' features (Fig. 1) [1]. Swiss cheese features have steep sides that grow outwards at a rate of a few meters per year [2], and it has been suggested that this growth could lead to a total resurfacing of the SPRC every ~100 years [3]. Swiss cheese features also have flat floors that could expose underlying water ice. We examine the potential atmospheric impact of Swiss cheese terrain temporarily uncovering water ice.

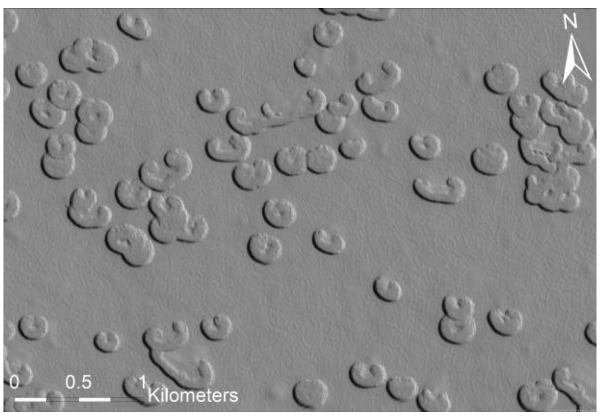

Fig. 1: Example Swiss Cheese features in the A1 Unit, from the Murray Lab Mosaic [8] at 86.9°S, 6.6°W.

This work is motivated by the 1969 (MY 8) Earth-based observation of an unusually high amount of water vapor (45-50 pr µm) over the south pole during southern summer [4]. Typically, the peak southern summer water vapor abundance is about 20 pr µm [5]. It has been suggested that the removal of most or all of the CO_2 ice of the SPRC, leaving exposed water ice to be sublimated, could be responsible for the 1969 observation [3, 6].

Our work estimates the magnitude of the impact Swiss cheese features may have on atmospheric water vapor, and if this is a plausible explanation for the unusual water vapor observation of 1969. We present results from mapping Swiss cheese features and a basic sublimation model to address these questions.

Mapping Swiss cheese features: In order to map individual Swiss cheese features on the SPRC, we used images from the Mars Reconnaissance Orbiter (MRO) Context Camera (CTX), which has a resolution of 5-6.5 m/pixel [7], in the Murray Lab mosaic in ArcMap, a blended mosaic of CTX images with a resolution of 5 m/pixel [8]. We used the Thomas et al. unit map (Fig. 1a in [1]) overlaid on the CTX mosaic to identify areas of Swiss cheese terrain.

Of the identified sites, those smaller than 0.5 km^2 were excluded because of the uncertainty in determining their exact margins. Due to the large total area of the unit, only those areas between 0.5-10 km^2 were mapped in their entirety, while for areas greater than 10 km^2, about 25% of the total area was mapped in order to derive a relative sample of Swiss cheese feature area versus high-standing CO_2 ice. Some Swiss cheese features contained interior raised areas ('mesas'). These are assumed to be CO_2-ice dominated remnants of the SPRC [9] and were excluded from the final total area of Swiss cheese features, allowing us to determine a fraction of terrain carved out of the SPRC by negative topography within each Swiss cheese site.

Sublimation estimation: We used surface temperature retrievals from the Mars Climate Sounder (MCS) to identify any secondary temperatures with a Swiss cheese terrain site. The MCS retrieval gave the brightness temperature of the whole scene. We used the surface pressure retrieval to calculate the CO_2 frost temperature within the scene and thus determine a scene emissivity. Scene emissivities greater than 1 indicated some material other than CO_2 also present within the scene, as a single component CO_2 surface cannot physically have an emissivity greater than 1. This secondary material was assumed to be water ice.

A linear subpixel mixing model was used to determine what temperature of water ice would be required to reproduce the retrieved MCS surface temperatures. From that derived water-ice temperature we determined a sublimation rate for the exposed water ice, assuming a sufficiently dry atmosphere and that sublimated water vapor is instantly transported away. We then calculated the column abundance of sublimated water vapor for the present configuration of Swiss cheese features, and then determined how much more exposed water ice is needed to recreate the 1969 observation.

Results: The total area of Swiss cheese terrain sites was 1628 km^2 of the total SPRC area of 86,572 km^2 [11]. The total mapped area of Swiss cheese features was 184.2 km^2, or about 0.2% of the total area of the SPRC.

14 sites met the criteria for MSC retrievals, which was narrowed down to five with scene emissivities greater than 1, indicating the presence of warmer water ice. Subpixel mixing plots were created for each of these sites, and lower-bound water-ice temperatures were determined. Five inferred water ice temperatures (Fig. 2) were above 190 K, much higher than the other inferred water-ice temperatures. The cause of these unusually high temperatures is unclear, and the temperatures were included in our calculations for completeness.

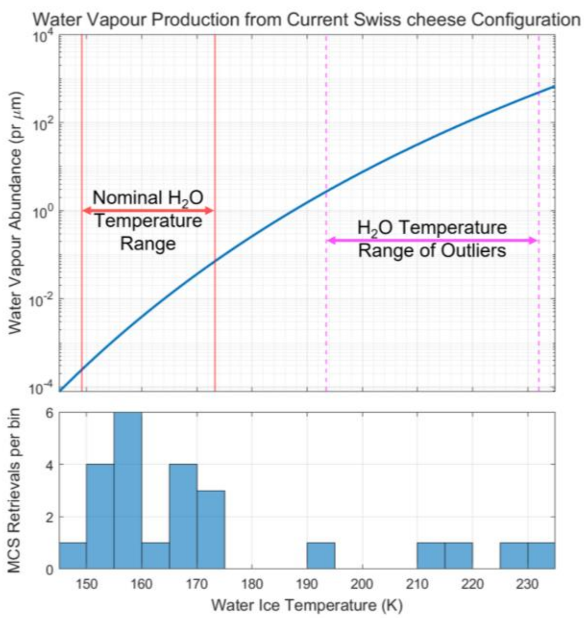

Fig. 2: Water vapor production for the current configuration of Swiss cheese features. Histogram of derived water-ice temperatures shows a clustering between 149-173 K, and five higher outlier values.

If we assume that the current total low standing area of Swiss cheese features exposes water ice which sublimates over the entire southern summer (154 sols), we see a maximum abundance of produced water vapor of 70.2x10^{-3} pr µm. This small quantity contributes insubstantially to the overall abundance of atmospheric water vapor. Additionally, the current configuration of Swiss cheese features could not have produced enough water vapor to account for the 1969 observation.

The 1969 observation saw a globally averaged water vapor abundance of 45 to 50 pr µm, more than 2 times the average southern summer abundance of 20 pr µm. Assuming that the nominal 20 pr µm are already present, we quantified the amount of Swiss cheese surface area needed to produce the remaining 30 pr µm. We assumed the same sublimation period and similar surface temperatures as those calculated for present day. At 173 K, the area of exposed water ice needs to increase by a factor of 427.2 to an area of 78 687 km^2, or 91% of the total area of the SPRC. At the lower limit of derived water-ice temperatures (149 K), the area requires is over 250 times that of the SPRC. However, these low temperatures would imply conductive equilibrium with the surrounding CO_2 ice, which can occur only for very thin veneers of H_2O ice.

Conclusions: The current configuration of Swiss cheese features account for around 0.2% of the total area of the SPRC. MCS retrievals for some of these Swiss cheese sites were indicative of the presence of water ice in late southern spring and summer. Assuming the entire mapped area of features exposes water ice, which then sublimates throughout the southern summer season, the globally averaged water vapor abundance produced (at maximum, 70.2x10^{-3} pr µm) is not enough to have an appreciable impact on atmospheric water vapor.

In order to bring this maximum vapor production up to levels seen in the 1969 southern summer, the area of water ice exposed by Swiss cheese features needs to increase to 91% of the total area of the SPRC. There is a sensitivity of water vapor production to temperature which suggests that relatively minor (~10 K) warming of water ice could have a significant impact on the total water vapor generated. Such warming could be driven by various environmental factors, leading to a higher sublimation rates for at least some part of the summer season.

Acknowledgments: This work was funded in part by the Natural Sciences and Engineering Research Council of Canada (NSERC) Technologies for Exo-planetary Science (TEPS) Collaborative Research and Training Experience (CREATE) program. The authors also wish to thank the Mars Climate Sounder project and the Murray Lab.

References: [1] Thomas, P.C. et al. (2009) *Icarus, 203*, 355-375. [2] Malin, M.C. et al (2001) *Science, 294*, 2146-2148. [3] Byrne, S. and Ingersoll, A.P. (2003) *Science, 299*, 1051-1053. [4] Barker, E.S. et al. (1970) *Science, 170*, 1308-1310. [5] Trokhimovskiy, A. et al. (2015) *Icarus, 251*, 50-64. [6] Jakosky, B.M. and Barker, E.S. (1984) *Icarus, 57*, 322-334. [7] Malin, M.C. et al. (2007) *JGR, 115*, E05S04. [8] Dickson, J.L. et al. (2018) *LPS XLIX*, Abstract #2480. [9] Buhler, P.B. et al. (2017) *Icarus, 286*, 69-93. [10] Hayne, P.O. et al. (2012) *JGR: Planets, 117*, E8. [11] Tanaka, K.L. and Scott, D.H. (1999) *Mars Geological Map of the Polar Regions, USGS*.